# LITERATURE REVIEW

This chapter provides an overview of the literature review regarding the synthesis, microstructural and tribological characterizations of copper based composites. Various authors have synthesized copper based composites by different techniques and reported its properties. Based upon the related type of work and literatures available, this chapter is organized in the different sub-section.

## 2.1 Composite materials and their classification

When two or more constituent materials are combined on a microscopic scale it results in a composite material whose physical properties are very different from the properties of individual constituents due to their synergy.

**2.1.1 Classification based on the reinforcement:** Schoutens et al. (1982) have defined the composites as:

**(a) Dispersion strengthened:** In this kind of composite uniformly distributed fine hard particulates, size in the range of 0.01 to 0.1 μm and in a volume percentage from 1 to 15 % are used to enhance the strength and hardness.

**(b) Particle reinforced:** Particle reinforced composite is almost similar to the dispersion-strengthened composite but the size of the particles is greater than 0.1 μm and the volume percentages can be greater than 25%.

**(c) Fiber reinforced:** Fiber reinforced composite includes all sorts of fibers, whiskers and filaments, continuous and non-continuous, over the entire range of concentration of the reinforcements.

### 2.1.2 Classification based on the matrix:

There are basically three types of composites in this category viz. (Fig.2.1).

(i) Ceramic matrix composites (CMCs)

(ii) Polymer matrix composites (PMCs) and

(iii) Metal matrix composites (MMCs)

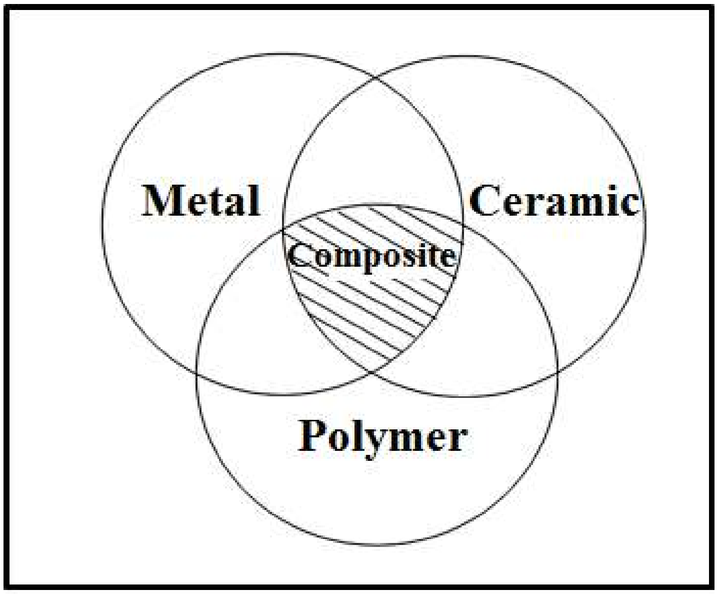


**Fig.2.1:** Classification based on the matrix used. [Source: M.Rosso (2006)]

**(i) Ceramic Matrix Composites (CMCs):** This class of composites contains ceramic materials as matrix phase. CMCs are developed primarily to improve the fracture toughness of ceramic materials. This makes the CMCs to be used in extreme environments of high temperature and stress state. The dispersed phase plays a major role in preventing the propagation of cracks. This dispersed phase can be fibers, particles or whiskers.

**(ii) Polymer Matrix Composites (PMCs):** They contain polymer as the matrix phase and fibers such as E-glass, carbon or aramid as the reinforcing phase. The different varieties of PMC mostly used are Glass Fiber-Reinforced Polymer (GFRP) composites, Carbon Fiber-Reinforced Polymer (CFRP) composites and Aramid fiber-reinforced polymer composites. The most commonly used polymers as matrix are vinyl esters and polyesters.

**(iii) Metal Matrix Composites (MMCs):** Metal Matrix Composites (MMCs), in general, consist of at least two components, one being a metal necessarily and other material may be a different metal or another material, such as ceramic or organic compound as reinforcement.

### 2.1.3 Classification of reinforcements used in metal matrix composites

It can be divided into five major categories.

a) Continuous fibres
b) Discontinuous fibres
c) Whiskers
d) Wires
e) Particulate

With exception of wires, which are metals, reinforcements are generally ceramics. Typically these ceramics are oxides, carbides and nitrides which are used because of their excellent combination of specific strength and stiffness at both ambient as well as at elevated temperature. Each of these reinforcements affects the base metal in different ways.

### 2.1.4 Advantages of metal matrix composites

Metal matrix composites (MMCs) have many advantages over monolithic metals such as:

a) Higher specific modulus
b) Higher specific strength
c) Better properties at elevated temperatures
d) Lower coefficients of thermal expansion
e) Better wear resistance

Because of these attributes metal matrix composites (MMCs) are under consideration for a wide range of applications. In comparison with most polymer matrix composites, MMCs have certain superior mechanical properties such as higher transverse strength, higher stiffness, greater shear strength, better compressive strengths and better high temperature capabilities. According to Rosso (2006) and Miracle (2005) these properties of MMCs are ideally suited for applications in automotive, aerospace and electronic sectors.

## 2.2 Processing routes to develop copper based metal matrix composites

The various processing routes are used to develop copper based metal matrix composites (MMCs), which can be categorized on the basis of temperature of the metallic matrix during processing as described by Rosso (2006). Accordingly, the processes can be broadly classified into five categories as shown in the Fig 2.2.

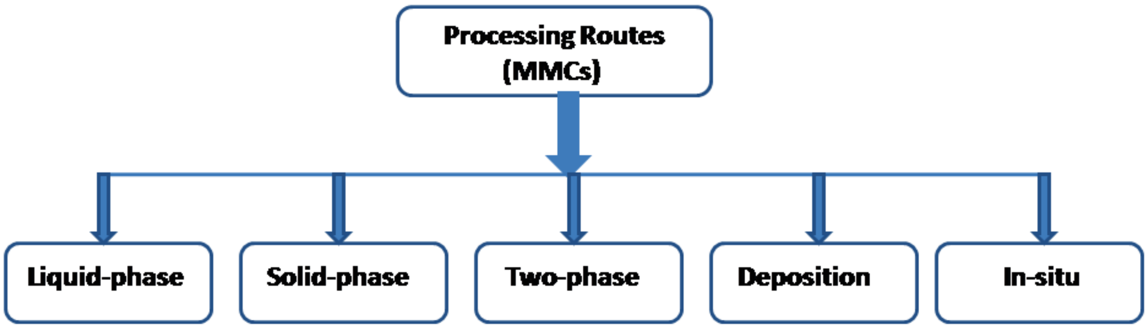


**Fig.2.2:** Classification of the processing routes to develop MMCs.

**2.2.1 Liquid phase processes:** The ceramic particulates are incorporated into a molten metallic matrix using various techniques. This is followed by mixing and casting of the resulting composite mixture into shaped components or billets for further production. There are three types of liquid phase fabrication methods: melt stirring; gas pressure infiltration and squeeze casting (Kainer 2006).

- Melt stirring: The matrix is taken in molten form to which the reinforcement such as particulates, whiskers or discontinuous fibers are added, thoroughly mixed solidified and then cut into required shapes. This technique is simple but involvement of high temperature during processing can damage the reinforcements.

- Gas pressure infiltration: In this process the melt infiltrates the preform with a gas applied from the outside. The advantage of this procedure is that there is no development of pores and this method can be used to produce large composite parts.

- Squeeze casting: This process is a forced infiltration technique of liquid phase fabrication of MMC, using a movable mold part (ram) for applying pressure on the molten metal and forcing it to go through into a performed dispersed phase, placed into the lower fixed mold part. The method is used for manufacturing simple small parts such as automotive engine pistons.

**2.2.2 Solid phase processes:** This process involves the fabrication of particulate reinforced MMCs from blended mixture of elemental powders and particulates. A number of steps prior to final consolidation are involved in these processes. Methods that fall in this category are: powder metallurgy and diffusion bonding.

- Powder metallurgy: The matrix and reinforcement are taken in the form of powders in proper proportion, mixed, heated and subjected to pressure causing diffusion to take place. This method is well suited for discontinuous fibre, whiskers and particulate reinforcements. One disadvantage is that there is loss of toughness when reinforcement increases over 50%. In case of powder metallurgy process the sintering can be performed by various techniques such as conventional sintering, spark plasma sintering and microwave sintering.

  Conventional sintering: In this process heating a preformed powder (raw or blended materials) at high temperatures is performed, although temperature is slightly lower than the melting point, during minutes to hours (ASM Handbook 1998).

  Spark plasma sintering: In which the material is heated by Joule effect and, a load applied on the material throughout the consolidation.

  Microwave sintering: Microwave sintering is closely related to dielectric properties, which are seen as indicators when materials are exposed to microwave irradiation.

- Diffusion bonding: In this process, a fibre matrix having fibres embedded in a polymer binder is kept between two sheets of matrix foil to form a ply. This can be consolidated or cut into smaller sizes, stacked together in a required sequence and then hot pressed to form the component. It is an expensive process but shapes such as tubes and plates are made by this technique.

**2.2.3 Two-phase processes**: This technique involves the mixing of ceramic and matrix in a region of the phase diagram where the matrix contains both solid and liquid phases. Two-phase methods are: spray deposition, compocasting / rheocasting.

- Spray deposition: In this process molten matrix metal is atomized and simultaneously sprayed with reinforcement powder on to a substrate. High production rates make the process economical (Srinivasan 2009).
- Compocasting / rheocasting: Uniform mixing can be achieved to a greater extent by allowing the melt to cool to a more viscous; two phase solid liquid state before stirring. The advantage of the process is that it is easy to mix particles more uniformly in a fluid of higher viscosity than in one of lower viscosity (Srinivasan 2009).

**2.2.4 Deposition techniques**: MMCs fabrication involve coating individual fibers on the matrix material to form the composite, followed by diffusion bonding to form a consolidated composite plate or structural shape. Various deposition techniques are: immersion plating; Chemical vapor deposition (CVD); Physical vapor deposition (PVD) (Rosso 2006).

- Immersion plating: Immersion plating is the process of applying adhering layers of nobler metals to another metal's surface by dipping in nobler metal solution ions to produce a replacement reaction. It causes the deposition of a metallic coating on a base metal from solutions that contain coating metal. This method is used to improve the wear resistance and electrical conductivity of the metal surface.
- Chemical vapor deposition (CVD): A substrate is placed in an even temperature furnace. The reactant gases are passed over it so that diffusion takes place. This method is simple and allows for using large furnaces to impregnate several objects at a time. The main disadvantage is that processing time is large.
- Physical vapor deposition (PVD): In this process the material goes from a condensed phase to a vapor phase and then back to a thin film condensed phase. This method is used to develop thin films and coatings. This method is used to produce semiconductor devices and coated cutting tools.

**2.2.5 In-situ process:** In these techniques the reinforced phase is formed in situ. The composite material is produced in one step from an appropriate starting alloy. Various advantages of in-situ process are that in situ synthesized particles and fibers are smaller than those in materials with separate fabrication of dispersed phase. Fine particles provide better strengthening effect. In situ fabrication provides more homogeneous distribution of the dispersed phase particles. The major disadvantage is that the choice of the dispersed phases is limited by thermodynamic ability of their precipitation in particular matrix (Aikin 1997).

## 2.3 Powder metallurgy method

Among these methods, the powder metallurgy (P/M) technique which is a solid state process is most appropriate to produce quality MMCs. Powder metallurgy is a well known processing technique over the last seven decades according to Torralba et al. (2003) for developing superior quality products which finds numerous important applications in power tools industry, aerospace, house hold appliances, electronics and much more. The powder metallurgy route is generally preferred due to various advantages such as:

a) Uniform distribution of reinforced particles which enhances its structural stability.
b) Dimensional control with an excellent surface finish
c) Mitigation of reactions between the matrix and the reinforcement.
d) Low-cost fabrication method for producing near-net shape composites.
e) The versatility of the P/M method is that it allows materials to be obtained which can not be obtained by any other processing route (i.e. SiC reinforcing Ti alloys).

### 2.3.1 Powder metallurgy processing

Figure 2.3 shows the various basic steps which involve during the powder metallurgy process.

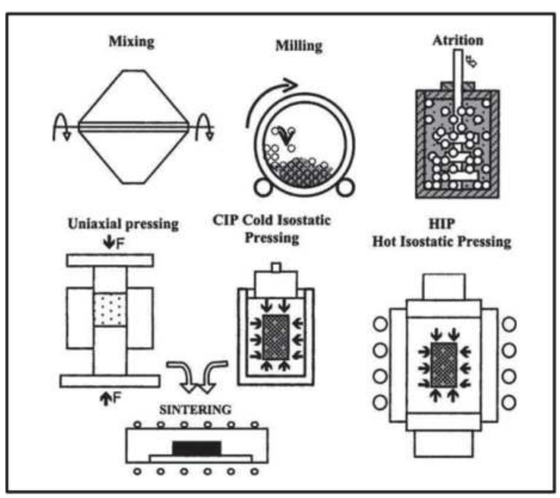


**Fig.2.3:** Various stages of powder metallurgy process. [Source: Torralba et al. (2003)]

### 2.3.1. (a) Mixing and blending

Mixing is carried out to achieve uniformity of the product manufactured. Distribution of the properly sized particles is attained by mixing elementary powder with secondary powders to obtain a homogeneous mixture. Lubricants are also mixed with powders to minimize the wear of dies and reduce friction between the surfaces of dies and the particles of powder during compaction. Mixing time depends upon the results desired, and over mixing should be prevented, or otherwise the size of particles will be decreased, and they will be hardened.

High energy ball milling is preferred over the conventional milling because it suppresses the agglomeration of the reinforcement particles when the size of the reinforcement is very small and results in homogeneous distribution of the reinforcement phase in the matrix. Planetary ball mill is a most commonly used system for mechanical alloying since only a very small amount of powder is required. Figure 2.4 shows the motions of the balls and the powder. Since the rotation directions of the bowl and turn disc are opposite, the centrifugal forces are alternately synchronized. Thus friction resulted from the hardened milling balls and the powder mixture being ground alternately rolling on the inner wall of the bowl and striking the opposite wall.

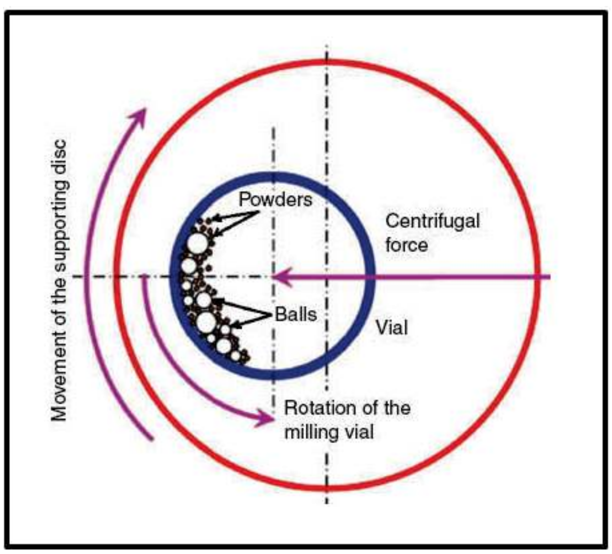


**Fig.2.4:** Schematic diagram of high energy ball milling.

#### 2.3.1. (b) Compaction

Compaction is generally performed at room temperature. Compaction process generates green strength of compacts by two phenomena: (i) particle sliding and interlocking, and (ii) plastic deformation as described by Narayanasamy et al. (2009). It was explained by Widanka (2008) that increasing applied pressure results in the increase of the density of the powder mass and decrease in its porosity. An attempt was made by Akbarpour et al. (2014) and Ahamed et al. (2011) to establish the relationship between applied pressure and density or porosity of the powder compact. The effect of applied pressure on the green density is shown by Fig. 2.5. Copper is relatively soft compared with iron, nickel and molybdenum powders and thus reaches a green density for a given compaction pressure. Copper and copper alloy powders are generally cold compacted in a closed die.

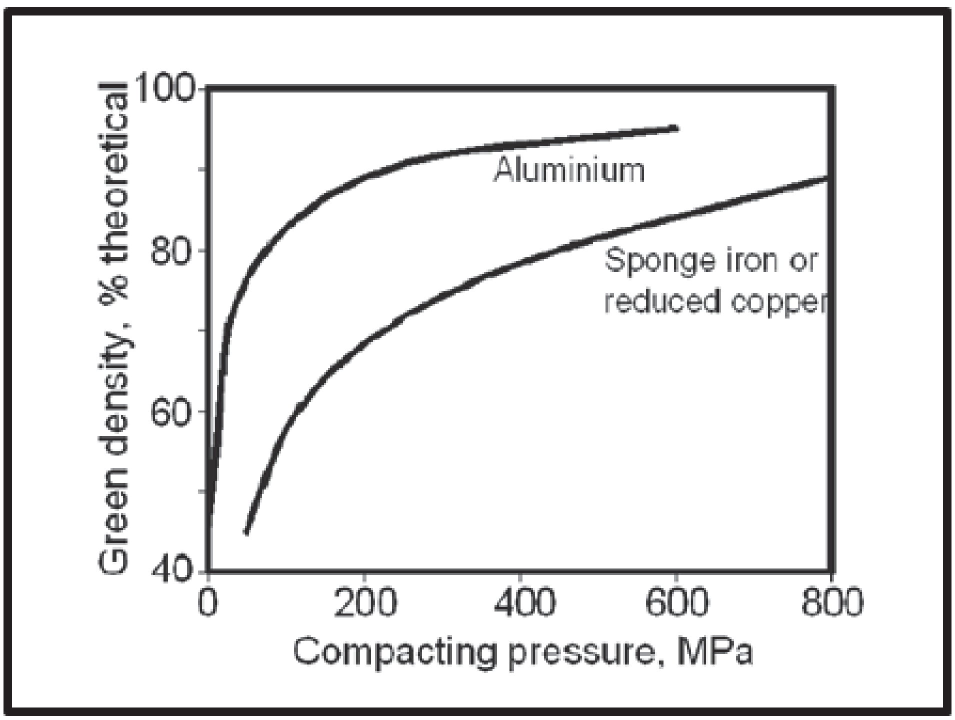


**Fig.2.5:** Relationship of green density and compacting pressure. [Source: Eksi et al.(2007)]

During the cold compaction, the powder particles mechanically interlock with each other. Typical compacted densities are 85 to 95 % of the theoretical density of the material.

#### 2.3.1. (c) Sintering

Sintering is the process in which powder compacts are heated, so that adjacent particles fuse together, imparting thus the strength and integrity. The temperature utilized for sintering is below the melting point of the major constituent of the powder metallurgy material. During sintering, particles fuse with each other and this phenomena result in the increase in the density of the compacts and hence the process is sometimes called densification. Figure 2.6 shows the process of diffusion during sintering. In course of sintering, particles get attached together and reduce the voids, resulting in dense structures with complex shapes.

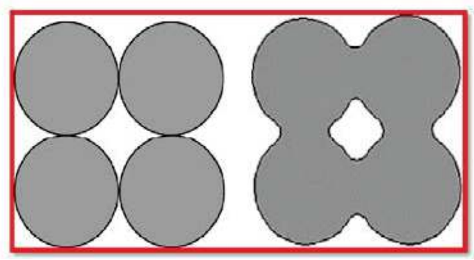


**Fig.2.6:** A schematic diagram of sintering. [Source: Eksi et al. (2007)]

## 2.4 Copper based metal matrix composites and their properties

### 2.4.1 Physical properties

Zhao et al. (2004) developed copper based composites reinforced by 9 vol.% WC following P/M route. Pure copper powder and 9 vol.% WC were blended in a milling machine for 48 h by using ceramic balls as the milling media. The weight ratio of ball to powder was about 5:1. Rotation speed was 200 rpm. Ethanol was used as a process control agent. The results show that the pressing process apparently influences the properties and microstructure of the composite. The properties improved with processing sequence progression and the uniform distribution of WC particles in the composite. It was suggested that pressing process can improve the bonding at the interface between copper and WC particles which can help in raising the critical stress for crack extension.

Copper based composites containing (0-3 wt. %) $Al_2O_3$ were developed via powder metallurgy method by Upadhyaya et al. (1995). In the investigation, the powders were prepared through the blending and mechanical alloying routes. The green compaction pressures were 500 and 560 MPa, respectively. Sintering of the green compacts was done in hydrogen at temperatures of 800°C and 900°C. Both sintered density and hardness were found to increase with increasing the compaction pressure. An increase in $Al_2O_3$ content resulted in increased hardness, with an associated loss in electrical conductivity.

Yeoh et al. (1993) prepared Cu-TiN composites by attrition and vibratory ball milling by conducting two separate experiments involving attrition and vibratory milling of Cu-3 wt. % TiN and Cu-25 wt. % TiN, respectively. The results showed that a layered morphology occurred in the attrition milled specimen, but not in the vibratory milled sample. Massive agglomeration was observed in the attrition milled powder, resulting in particle sizes larger than the starting powder sizes. In the vibratory milled case, excellent powder particle refinement occurred and nano size copper and titanium nitride particles were observed under TEM. It was pointed out that vibratory milled powder did not cause much grain growth of the copper particles. The observed behavior has been credited to the high volume fraction of TiN which caused large scale grain growth.

Dash et al. (2016) investigated the implications of degree of thermal shocks on flexural properties of copper with 1, 3, 5, 7 vol.% alumina nano-composites and with 5, 10, 15, 20 vol.% micro-composites fabricated by conventional powder metallurgy route. Down-thermal shock treatments enhance the ultimate flexural strength of Cu- $Al_2O_3$ micro- and nano-composites. Up-thermal shock treatment (-40 to +40 $^oC$ temperature) enhance the ultimate flexural strength of Cu-$Al_2O_3$ nano-composites. SEM micrographs reveal ductile mode of fracture for micro- and quasi- cleavage for nano-composites. Failure analysis reveals particle pull-out, crack entrapment, and physical outgripping of alumina particles as the operative mechanisms during fracture.

Copper matrix composite reinforced with $Y_2W_3O_{12}$ by high energy ball milling followed by compaction and sintering were prepared by Das et al. (2014). The relative density of the composites was found to be around 90% for the 10 h milled powders followed by compaction at a pressure of 700 MPa and sintering at a temperature of 1000°C. The thermal expansion of the composites exhibited linear behavior in the temperature range from 200 to 800°C and the low coefficient of thermal expansion (CTE) was observed for Cu–70%$Y_2W_3O_{12}$.

Sorkhe et al. (2014) determined the electrical conductivity of $TiO_2$ (0, 1, 3, 5 and 7 wt. %.) reinforced copper composite by using four probe technique. They observed that the electrical conductivity decreases with the increase of mass fraction of $TiO_2$ particles. It was also suggested that low electrical conductivity of the oxide particles is not the only reason of the decrease in electrical conductivity of the composite. Significant contribution also results from the scattering of the conduction electrons which occurs due to the large number of dislocations produced during the milling process and presence of porosity.

Rajkovic et al. (2008) investigated the properties of copper matrix reinforced with nano and micro-sized $Al_2O_3$ particles. High energy ball milling was employed to produce nano composites. It was noticed that micro hardness of nano size reinforced composites was 3.6 times higher than the micro sized reinforced composites. Electrical conductivity of high energy milled composites was found to be better than the non milled composites.

Efe et al. (2012) investigated the effect of SiC particle size on Cu-SiC composites developed via powder metallurgy route. It was observed that mechanical properties enhances with 1, 2, 3 and 5 wt.% SiC addition. The SiC particles are of 1, 5 and 30 µm sizes. They found that the conductivity depends on the particle size and amount of reinforcement. Electrical conductivity of composites was found to decrease with increasing weight percentage of SiC content and the coarse particles were good in maintaining the electrical conductivity than fine particles.

Yusoff et al. (2011) developed the nano-structured tungsten carbide-reinforced copper composite produced via mechanical alloying followed by compaction and sintering. Cu-30 vol.% WC was mechanical alloyed for 0-60 h. Hardness of the composites increases with increase in WC. A significant decrease in electrical conductivity after 20 h milling resulted from the scattering of the conduction electrons as a result of a large number of dislocations. In addition, the grain boundary volume increased, thus generating more barriers against the conductive path.

Bagheri et al. (2014) prepared Cu-TiC nano-composites by high enery ball milling followed by compaction and sintering. In this investigation, powder mixture Cu-40 wt.% Ti were milled for 60 h, then graphite powder was added, consequently milling was continued for further 10 h. The sintering of the compacted specimens takes place at 900°C. XRD patterns show the presence of TiC in the composite. The lattice parameter, crystallite size and lattice strain was determined using Nelson-Riley method and Williamson-Hall equation after different times of milling. It was found that the lattice parameter of Cu increases upto 60 h of milling and then decreases with further milling. The increase in lattice parameter can be credited to the solid solution formation in early stage of milling. Whereas, the decrease in lattice parameter after 60 h of milling can be due to exit of Ti atoms from Cu lattice and the formation of TiC particles. Crystallite size decreases from 63 nm to 11 nm after 70 h milling and this can be due to the severe deformation of powder particles subjected during milling. Similarly, the increase in lattice strain can be due to cold work effect and formation of lattice defects like vacancies, dislocations and stacking faults.

Oanh et al. (2015) studied the synthesis and characterization of Cu-TiC composites. In this investigation Cu (99% purity, 75 µm) were taken as a matrix and TiC particle ( 30-45 nm, Alfa Aesar) were added in 5, 10, 15 wt. % into the copper matrix. The powder mixture of Cu and TiC was milled at rotational velocity of 400 rpm for 5 h. After the milling compaction and spark plasma sintering (SPS) takes place at 600°C and 700°C. From XRD analysis peaks of Cu and TiC were detected. The peak intensity is lowering with increasing TiC content and it can be possibly due to the hindering of grain growth by fine TiC present in the matrix during sintering. Relative density decreases with increase in TiC content and this can be credited due to the of hard, non deformable TiC particles, which hinder the plastic deformation during SPS process. Hardness increases with increase in TiC content. The reason was that TiC reinforcement would share the most of the load when an external load is applied. It is also an indication of good interfacial contact between reinforcement and matrix.

Wang et al. (2014) developed TiC-dispersion-strengthened Cu alloys by a two-step ball-milling (BM) process followed by sparks plasma sintering (SPS), heat treatment and hot rolling. The starting materials were electrolytic copper (99.9% purity, 45 μm), graphite (99.7% purity, 1 μm) and titanium (99.9% purity, 38 μm). In the first step Ti and graphite were pre ball milled and were followed by a second-step BM with Cu powder for a designed composition (mass%, Cu–2.4Ti–0.6C). In this study, three cases designated as high ball to powder ratio (BPR)-low rpm (rpm: 300 and BPR: 5:1), low BPR-high rpm (rpm: 600 and BPR: 1.5:1) and high BPR-high rpm (rpm: 600 and BPR: 5:1) were chosen for investigation of pre milled Ti and C. Samples taken out of the vial at intervals of 1 h, 2 h, 4 h and 8 h. In second step milling was with Cu at 600 rpm for 1.5 h under argon atmosphere. After this the compaction takes place followed by SPS at a temperature of 1123 K and pressure of 40 MPa under the high level vacuum atmosphere. The XRD and microstructure analysis revealed that the transformation of Ti and C into TiC can be achieved during pre-BM with high BPR-high rpm condition and it results in higher electrical conductivity but much lower strength compared with the case with high BPR-low rpm and low BPR-high rpm where TiC in-situ formed during sintering and heat treatment. The residual Ti in Cu matrix was found to be the predominant factor lowering the electrical resistivity of Cu–Ti–C alloys compared with other influence factors such as grain boundaries, dislocations and pores.

Zarrinfar et al. (2004) developed Cu–TiCx master-alloys by reaction synthesis of elemental powder mixtures. They explored the wettability between the reactants and metallic matrix. Titanium powder with a particle size between 125 and 180 μm and >99.5% pure and graphite <10 μm in size and >98.5% pure, were used as reactants to form TiCx by SHS. Copper powder <75 μm in size and >99.7% pure, was used as the metallic matrix. To produce the master-alloy, appropriate amounts of titanium and carbon powders were weighed accurately to give different C/Ti atomic ratios between 1 and 0.3. The graphite crucible and its contents were heated in an induction furnace to $1200^{o}$C to melt the copper pieces and the master-alloy. It was found that the successful incorporation and dispersion into molten copper occurred when the C/Ti ratio in the reactants was <0.50.

Chandrakanth et al. (2010) developed copper based hybrid composites reinforced with TiC and graphite particles through microwave processing. In this investigation electrolytic copper powder (99.5%, 12 μm) were taken as matrix material whereas graphite (99.8%, 50 μm) and TiC (99.2, 11 μm) were taken as reinforcements. The content of graphite was 5 and 10 vol. % and TiC was 5, 10, and 15 vol. %. The sintering of the specimens was performed at 700, 800 and 850°C. Thermal gravimetric analysis of Cu–TiC (15 vol. %)– graphite (10 vol.%) mixture suggested that ramp rate of 12°C/min and 800°C is suited for sintering since no weight loss/ degradation occurred. It was observed that the increase in sintering temperature and isothermal holding time increases the relative density. It was also observed that no remarkable change in sintered density is observed with the increase of sintering temperature from 800°C to 850°C. Microstructural analysis shows the uniform distribution of the TiC and graphite reinforcements. EDS analysis shows the presence of C, Ti, and Cu. When the graphite percentage is increased, the increase in porosity is observed. This is due to the tendency of the formation of agglomerates. The hardness of the hybrid composites increases with increase in TiC content and it may be credited to TiC reinforcement which would share the most of the load when an external load is applied.

Xiao et al. (2007) studied the development of TiC-Cu cermets by using self-propagating high-temperature synthesis. In this investigation, 40 wt.% titanium powder (135-154 μm), 10 wt.% carbon black (0.033-0.079μm), and 50 wt.% copper powder (135-154 μm) were mixed thoroughly and compact were made. This compact was ignited in a reaction chamber at 1832 K and the combustion wave self-propagated through the compact from top to bottom. XRD pattern of the combustion-synthesized product indicates that the product consists of TiC and Cu phases. It was found that with an increase in temperature, more and more Ti and Cu as well as C particles were dissolved into the Ti-Cu liquid solution forming Ti-Cu-C liquid, and TiC particles began to precipitate in the saturated Ti-Cu-C solution. SEM results show the precipitation of TiC particles in the saturated solution.

Jie et al. (2012) reported the effect of process parameters on the microstructure and properties of TiC reinforced Cu-matrix composites. Electrolytic copper powders（74 μm, purity > 99.5%) were reinforced with different wt.% of TiC (5, 10, 20, 30, 40, and 50). The raw powder were mixed and grinded by high-energy ball milling with rotating speed 500 rpm/min under argon atmosphere for 6 h, 15 h, 24 h respectively. After that the compacted specimens were sintered at 1000°C and 800°C for 60 min in a tube vacuum furnace. It was observed from the SEM analysis that 24 h ball milled composite particles shows the thinner and more active particles which appear as the aggregation and the grain growth occurs. It was analyzed that plastic deformation and cold welding occur in powders at the early time of the ball milling. Density of the ball milled composites is higher than the composites without ball milled. As TiC content changes from 0 to 50 wt. %, the bend strength increased first and then decreased. It was observed that electric conductivities decrease with the increase in TiC content.

Liang et al. (2008) reported the evolution process of TiC formation in the 20 wt.% Cu–Ti–C powder mixtures by using differential thermal analysis (DTA), X-ray diffraction (XRD) and scanning electron microscopy (SEM). It was observed by DTA and XRD analysis that evolution process of TiC formation in the following ways: the $Ti_xCu_y$ compounds ($Ti_2Cu$, TiCu, $Ti_3Cu_4$, and $TiCu_4$) formed initially via the solid state diffusion reactions between the Cu and Ti and then the $Ti_2Cu$ and TiCu can form the Cu–Ti eutectic liquids at about 1233 K. The unreacted Ti and C particles dissolved into the Cu–Ti liquids and led to the formation of the Cu–Ti–C ternary liquids; subsequently, TiC formed in the liquid.  Microstructural results are in agreement with the XRD results.

Hoang et al. (2017) prepared TiC–Cu composites containing 20 and 30 vol.% of nano-sized titanium carbide (TiC) by powder metallurgy using copper powders with micrometer-sized and nanometer-sized particles. Copper powder (75 μm and 40 nm) and TiC powder (40–60 nm) was ball milled for 10 h and spark plasma sintered at 800–900$^{o}$C under an applied pressure of 50 MPa. The crystallite size of the copper matrix in the composites prepared using the nanometer-sized copper powder was smaller than in composites prepared by using the micrometer-sized copper powder, which was confirmed by transmission electron microscopy (TEM). From XRD it is clear that between Cu and

TiC, no copper oxides were found in the sintered nano-composites. The hardness of the composites increased as the sintering temperature was increased from 800 to 900$^{o}$C.

Zhuang et al. (2009) studied the microstructural characterization of the Cu-Ti-C composites prepared by mechanical alloying and spark plasma sintering. Copper (purity 99.9%, 44 μm), Ti (purity 99.9%, 44 μm) and graphite (purity 99%, 26μm) are selected as starting element powders. The Ti and graphite powders were mixed with the atomic ratio of 1:1, the Cu composition was 50 wt.% and 70 wt.% in this experiment. The high energy ball milling was done for 20 h and the speed was 500 rpm. The spark plasma sintering was done at a sintering temperature of 850$^{o}$C, 900$^{o}$C, 950$^{o}$C, 1000$^{o}$C and 1050$^{o}$C, separately. It can be seen from XRD spectrum that TiC peaks with low intensity appeared when the samples were sintered at 850$^{o}$C. $Ti_2Cu_3$ peaks were found at 1050$^{o}$C. It was observed that TiC formed from the Ti which solved in the Cu matrix during milling. Carbon peak appeared when sintering temperature was 950$^{o}$C, $Ti_2Cu_3$ peaks were found at 1050$^{o}$C. The heating duration is for 3 minutes. Both density and microhardness of specimen increased at first by densification, but decreased after rising sintering temperature, because part of Cu was squeezed at higher temperature.

### 2.4.2 Mechanical properties

The effect of SiC content on the hardness, electrical conductivity, density and coefficient of thermal expansion (CTE) of Cu–SiC composites produced via high energy ball milling was studied by Prosviryakov (2015). It was shown that an increase in milling time and SiC content (up to 25 wt. %) led to a higher hardness of the materials due to homogenization of the microstructure and refinement of the reinforcing particles. However, an increase in SiC content over 25 wt. % decreased the hardness due to severe reduction of the microstructural homogeneity and an increase in the porosity of compact specimens.

Khisamov et al. (2015) investigated the microhardness and microstructure of carbon nanotubes (4 wt. %) reinforced copper composites produced via powder metallurgy. It was pointed out that that the matrix grain size after severe plastic deformation significantly decreases, while the internal stress level, dislocation density, and composite microhardness increases with increasing concentration of nanotubes.

Gao et al. (2016) investigated the mechanical and thermal properties of grapheme reinforced copper matrix composites. Gr/Cu composites with different graphene contents were prepared by electrostatic self-assembly and powder metallurgy. It was observed that graphene is homogeneously distributed in the Cu matrix and no evident agglomeration of graphene is observed. As a result, the UTS, Vicker hardness and thermal conductivity of the composite initially increase and later decline. When the graphene content is 0.3 wt.%, the UTS and thermal conductivity of the composites reach the highest.

Yue et al. (2017) developed the graphene nano sheets (GNSs) reinforced pure copper matrix composites by ball-milling followed by hot-press sintering. It was pointed out that the GNSs are gradually dispersed into the copper matrix with increasing the ball-milling time and thus a uniform dispersion is achieved after ball-milling for 5 h. It was also observed that when the content of GNSs in the composite is 0.5 wt.%, then GNSs distribute randomly in the composite and results in good interface bonding which increases the mechanical properties of composite

The effect of milling and sintering techniques on mechanical properties of Cu–graphite metal matrix composite prepared by powder metallurgy route was explored by Samal et al. (2013) by using conventional and spark plasma sintering (SPS). The relative densities of 90% and 97% were obtained for conventional sintered and SPS samples, respectively. The maximum Vickers hardness value of around 70 and 100 are achieved for Cu–1 vol.% graphite reinforced MMC. The transverse rupture strength increases up to 5 vol. % of graphite reinforcing and after that it decreases.

Nayan et al. (2017) developed copper matrix composites reinforced with 0.2, 5 and 10 vol.% single walled carbon nanotubes (SWCNT) and 5 and 10 vol.% multi-wall carbon nanotubes (MWCNT) through high energy ball milling followed by spark plasma sintering. From Raman spectroscopy it was noticed that there is an increase in number of defects in the nano-tube after milling and sintering of the composite. It was observed that mechanical properties (strength and deformability) are better for SWCNT composites compared to MWCNT. The failure strain decreases with increase in volume percent of CNT due to clustering of CNTs.

Altinsoy et al. (2013) synthesized Cu-$B_4C$ composites by high energy ball milling followed by compaction and sintering. The sintering of the compacts was done at 700$^oC$ for 2 h in open atmosphere before being subjected to cold pressing. Scanning electron microscope (SEM-EDS) showed that $B_4C$ particles are distributed homogenously in the copper matrix. The relative densities of Cu and Cu-$B_4C$ composites ranged from 97.5% to 90.19%. It was found that micro-hardness of composites ranged from 80.65 to 87.5 HB and the electrical conductivity of composites changed between 90.04 % IACS and 68.87 %IACS.

Tomolya et al. (2017) studied the synthesis and characterization of copper-based composites reinforced by CuZrAlNiTi particles. The reinforcement was added in 30, 40 and 50 wt.% into the copper matrix. The composites were high energy ball milled at 1000 rpm for 10 min. It was observed that compressive strength and yield strength of copper increases with increase in reinforcement content.

The compaction behavior of Cu/SiC composites prepared via mechanical alloying was studied by Gan et al. (2008). In this investigation 30 vol.% of SiC and 70 vol.% of Cu powder were taken and mixed in a steel jar at milling speed of 600 rpm while keeping a BPR of 10:1. The powders were milled for 0- 10 h and compressed at pressures between100- 800 MPa. The shape of the copper was observed to change from dendritic to spherical with the increase in time of milling. It was observed that the morphology and hardening effects during ball milling affects the compressibility behavior of the powders. The compressibility of powders was observed to vary linearly with the compaction pressure and density of the powder in accordance with the equation proposed by Panelli and AmbrosioFilho (2001).

Akbarpour et al. (2014) investigated the microstructure and compressibility of SiC nano-particles reinforced copper nano-composite powders prepared via high energy mechanical milling and explored the effects of SiC content and milling time on apparent density (AD) and tap density (TD) of the nano-composite powders. The compaction data were fitted to the Panelli–Ambrosio Filho equation in order to examine the influence of mechanical milling time and SiC content. They observed the changes in powder morphology and hardness with increasing milling time and concluded that the major mechanism for densification at higher mechanical milling time was the particles rearrangement.

Li et al. (2001) explored the effect of titanium carbide (TiC) on the performance of sintered copper-based materials as electrical discharge machining (EDM) electrodes. Six batches of titanium carbide with content from 5% to 45% were fabricated by mixing, ball milling, pressing, and liquid phase sintering with copper-tungsten (Cu-W) and copper Cu, respectively. The densification of TiC/Cu-W system was improved by the addition of nickel Ni, as Ni shows good solubility in both Cu and W. It was observed that with increasing TiC, the relative density first increased and then decreased, whereas the electrical resistivity first decreased and then increased. It was concluded from the investigation that EDM electrodes, with the addition of TiC, show good performance in surface finishing.

Akhtar et al. (2009) developed high volume TiC reinforced Cu-matrix composites by powder metallurgy method. They investigated its microstructure, mechanical properties, electrical conductivity and wear behavior. Both TiC and Cu powders were wet milled in ethanol for 48 h. The milled powders were poured into the die and pressed uniaxially at 500 MPa pressure. The prepared green compacts were sintered in a temperature range from 1200°C to 1350°C for 1 h in vacuum. The microstructural study of the composites revealed that the titanium carbide particles were distributed uniformly in the matrix phase. No interface debonding and micro-cracks were observed in the composite.

The effect of the TiC content on the microstructure and thermal properties of Cu–TiC composites prepared by powder metallurgy was investigated by Buytoz et al. (2014). The different amount of TiC (1, 3, 5, 10, and 15 wt.%) were reinforced into the copper matrix. The Cu–TiC powder mixtures were hot-pressed for 4 min at 700$^{o}$C under an applied pressure of 50 MPa. From microstructural studies it was found that TiC particles were homogeneously distributed in the Cu matrix as shown in Fig.2.7. With the increasing content of TiC, hardness of composites changed between 58.6 $HV_{0.1}$ and 87.8 $HV_{0.1}$. It was also observed that electrical conductivity decreases with increase in TiC content.

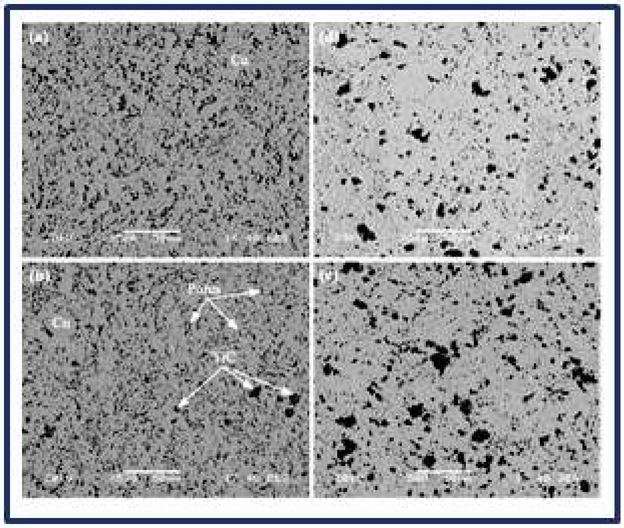


**Fig.2.7:** Microstructure showing the dispersion of TiC in Cu matrix. [Source: Buytoz et al. 2014]

Sabbaghian et al. (2014) prepared TiC reinforced copper-based composite via friction stir processing and reported a good bonding between reinforcing particles and base metal. The maximum hardness in the stir zone was found to be 117 Vickers which was higher in comparison to the hardness of pure copper which was 65 Vickers. X-Ray analysis confirmed the absence of inter-metallic compounds in the stir zone.

Cu-TiC composites by powder metallurgy method were successfully synthesized by Islak et al. (2014). Pure copper powder (20 μm) and titanium carbide powder (10 μm) were used as a starting material. Copper matrix was reinforced with TiC (10 wt.%). Cu-TiC powder mixtures were hot-pressed for 4 min at 600, 700 and 800°C under an applied pressure of 50 MPa. Phase determination and microstructure of the composites hot pressed at different temperatures were characterized by X-ray diffraction, scanning electron microscope, and optical microscope techniques. Microstructure analysis revealed that TiC particles were uniformly distributed in the Cu matrix. Hardness of composites changed between 64.5 $HV_{0.1}$ and 85.2 $HV_{0.1}$.

The densification, workability and strain hardening behavior of sintered copper and Cu–7.5% TiC produced by powder metallurgy (P/M) were explored by Narayanasamy et al. (2008). The effects of aspect ratio and addition of titanium carbide with copper on the formability behavior and various constants involved in the constitutive model, namely, instantaneous density coefficient, instantaneous strain hardening index, instantaneous strain rate sensitivity and instantaneous strength coefficient were discussed in detail. It was reported that during the first stage of densification the plasticity range has been significantly increased for Cu–7.5% TiC, because there is a significant increase in the stress ratio. A relationship between the stress and relative density was established.

Vu et al. (2012) developed Cu-TiC composites containing 1-5 wt.% of TiC using powder metallurgy route. It was pointed out that with increase in TiC content relative density decreases. It was also noticed that tensile strength increases upto 2 wt.% TiC content. Beyond the 2 wt.% TiC content the tensile strength decreases due to the agglomeration of TiC particles. Electrical resistivity increases with increases in TiC content.

Rathod et al. (2013) studied the effect of aluminium addition on densification behavior and micro structural features of P/M processed Cu–TiC composites and found that increase in aluminium and TiC contents lead to a better chemical homogeneity in the composites. Separate addition of Al and TiC to copper results in the increased hardness. Further, the hardness of the samples increased with the addition of aluminium content while a mixed effect of TiC content was noticed. It was further suggested that aluminium addition is more effective at a higher TiC content in terms of increased hardness of the samples.

Wang et al. (2016) investigated the hot deformation behavior of TiC-strengthened copper composite (Cu-5 vol.% TiC) by combination of mechanical milling and spark plasma sintering (SPS). The SPS process was performed at the temperature of 800°C and pressures of 40 MPa for 5 min under a high level vacuum atmosphere. The stress-strain curves in all conditions were characterized by a fast increase in stress at initial stage and a subsequent yield drop. No obvious microstructure change was observed with increasing reduction ratio. There exhibited a tendency in grain size refinement with increasing strain rate even the change in grain size is slight. The high temperature tensile tests results suggested that the yield stress showed a relatively weak dependence on strain rate with a strain rate sensitivity parameter of around 0.02, and a low degree of strain hardening was observed. The fracture morphologies occurred during the tensile test was closely related to the change in particles distribution from random to aligned distribution during the hot press deformation.

Harish et al. (2015) synthesized copper based TiC reinforced in-situ metal matrix composite by melting copper, hexaflurotitanate and graphite powder in appropriate proportion at a temperature of 1100$^{o}$C using stir casting technique. The maximum weight percentage of reinforcement was limited to 10 wt.%. X-ray diffraction analysis confirms the formation of titanium carbide particles. It was found that developed composite exhibit a significant improvement in hardness and ultimate tensile strength compared with unreinforced copper.

Palma et al. (2005) studied the performance of a nominal-composition Cu–5 vol.% TiC alloy prepared via powder metallurgy and evaluated its application as electrodes for electrical-resistance welding. Cu (40µm), Ti (45µm) and graphite powders (6 µm) were taken as a raw material to form Cu–5 vol.% TiC alloy using hexane as milling media. The flakes obtained by milling were encapsulated under low vacuum and then consolidated by extrusion at 1023 K, using an extrusion ratio of 10:1. Electrodes performance was evaluated by means of the following indexes: tip shortening, tip widening, and mass loss. Electrolytic copper electrodes were used as reference. The results obtained clearly demonstrate that the Cu–TiC electrodes prepared from powders synthesized by reaction milling have a remarkably better performance than those manufactured from electrolytic copper.

Bagheri (2016) investigated the effect of TiC reinforcement on copper based composites. In this investigation reinforcement were produced via mechanical alloying and in-situ formation. Copper, titanium and graphite powders with particle size of less than 63 µm were used as starting materials and these powders were milled in a planetary ball mill for 60 h. Changes in lattice parameter, crystallite size, lattice strain, dislocation density and Gibbs free energy changes were studied by using X-Ray Diffraction technique. Mechanical properties increases with increasing the TiC content

Chrysanthou et al. (1996) worked on enhancing the dispersion of TiC in copper with the help of Nickel. It was observed that nickel with its incomplete 3d orbital acts as an acceptor of electrons. It was concluded that addition of nickel to copper can enhance the degree of dispersion of TiC.

A critical review of above mentioned literature makes it evident that authors have worked on the various ceramic reinforced copper composites. Few authors have also reported their work on the titanium carbide particles reinforced copper matrix composites and explored their synthesis, compaction and hardness behaviors. However, there is a lack of work reported on the Cu-4 wt.% Ni matrix alloy reinforced with TiC and its various characteristics.

## 2.5 Frictional behavior of composite materials

Friction is defined as the resistance to relative sliding between two bodies in contact under a normal load. The frictional force arises due to the interactions between the opposing asperities of the two mating surfaces. Each asperity interaction contributes to the friction force thus; the total friction force at any time is the sum of the forces at the individual asperity contacts. The Coulomb (1785) has proposed the basic laws of friction which are given below:

**First law**: Friction is independent of the normal load.

**Second law**: The friction force is independent of the apparent area of contact between the contacting surfaces.

**Third law**: The kinetic friction force is independent of the sliding velocity, once motion starts.

### 2.5.1 Theories of Friction

The theories of friction can be summarized as:

**Adhesion theory:** Bowden and Tabor (1950) proposed the adhesion theory of friction which states that adhesion is a surface interaction mechanism and ability of contacting bodies to oppose tensile forces after being pressed with each other. A strong adhesive junction is formed when two precise clean surfaces are pressed together. No inter-diffusion or re-crystallization of metal atoms takes place at the junction, as is done in a cold condition and the condition predominating at the interface of the junction is like "cold welding".

**Asperity interlocking theory:** In engineering surfaces, it is practically not easy to get a perfectly smooth and flat surface. It has some asperities and waviness. When two surfaces are placed in contact with each other, they touch only at discrete points called asperities. The applied load is supported by the deformation of the contacting asperities. Among many investigators, Coulomb (1736-1803) was perhaps the first to develop a model, to understand the friction due to the interlocking of asperities. During sliding, the plastic deformations of softer asperities have to take place by the application of force. This leads to frictional resistance.

**Molecular attraction theory:** Hardy (1928) was the first to state that friction is because of the molecular attraction. The origin of this theory is the partial irreversibility of the bonding force among the atoms. Such molecular attraction works over short distances and thus discriminates between the real area of contact and apparent area of contact. Still, this theory may perhaps be considered to have a certain scope as the "adhesion theory".

**Stick-slip theory:** Bowden and Leben (1939) were first to coin this term. It may also be considered as an alternative description of the adhesion theory. The assumption is that one surface rests over another at junctions. As soon as one surface starts sliding over another, a rise in temperature occurs at these junctions; this results in local welding at the point of contact (junction). Therefore, it leads to a resistance to motion, i.e., friction. Sliding occurs on account of applied force, by the tearing apart of these welds. Proximately, after this sliding, local welding takes place on another set of junctions, which are again torn to enable sliding and such sticking and slipping (sliding) continues.

### 2.5.2 Factors affecting the friction behavior of composites

According to Coulomb, the various factors which can influence the friction are:

a) The nature of the materials in contact and their surface coatings

b) The extent of the surface area

c) The normal load, and

d) The duration of time that the surfaces remained in touch.

Friction between two rubbing bodies is not independent of the velocity as suggested by Coulomb (1781). Rabinowicz (1965) and many other researchers have shown that friction is a function of sliding velocity and not dependent on the load alone. Rabinowicz (1965) has indicated that a drop in friction is universally observed as sliding speeds are raised to high values due to the thermal softening of the interface, resulting in lower shear strength of the interfacial layer while maintaining the substrate at almost the same level of hardness. Suh et al. (2008) observed that frictional behavior of the composites was assumed to be somewhat influenced by their comparatively high surface roughness of 1µm in case of copper composites. During the steady state, the average frictional coefficient value was apparently lower for the indium doped copper composite than for the composite without indium. Kovalchenko et al. (2012) pointed out the frictional behavior of Cu based composites containing $MoS_2$ and $MoSe_2$. In the investigation it was found that at the initial stage of sliding, before scuffing, the coefficient of friction showed a steady value of approximately 0.2. There was little noise, and the wear tracks were smooth, showing no sign of surface damage. However, when scuffing occurred with the sudden rise in the coefficient of friction, a loud audible noise and vibration were observed. As a result, the worn surfaces of the pins and plates appear highly deformed, smeared and torn. Celikyurek et al. (2011) found that the coefficient of friction of Cu increased with increasing sliding speed whereas the coefficient of friction of composites decreased with the increase in sliding speed. It was reported by Akhtar et al. (2009) that for Cu-TiC composites coefficient of friction increases with increase in load. Similar observation of increase of coefficient of friction with increases in load for Cu-graphite-TiC composites was observed by Rajkumar et al. (2011).

Rabinowicz (1965) suggested that for very smooth surfaces, the friction tends to be high because of larger real area of contact, whereas with very rough surfaces the friction is high because of the need to lift one surface over the asperities on the other. But in the intermediate range of surface roughness normally used in the engineering surfaces, the friction is almost constant and independent of the roughness of the surface.

## 2.6 Types of wear

Wear is correlated to interactions between surfaces and more precisely, the removal and deformation of a material on a surface as a result of the mechanical action of the opposite surface (Rabinowicz 1995). In other words, wear is defined as the progressive loss or undesired removal of materials from a surface. The various types of wear are (i) adhesive wear, (ii) abrasive wear, (iii) erosive wear, (iv) fatigue wear, and (v) corrosive wear.

**Adhesive wear** is a result of micro-junctions caused by welding between the opposing asperities on the rubbing surfaces of the counter bodies (Rabinowicz 1995). The load applied to the contacting asperities is so high that they deform and adhere to each other forming micro-joints. The motion of the rubbing counter bodies result in rupture of the micro-joints. The welded asperity ruptures in the non-deformed regions. Thus, some of the material is transferred by its counter body. This effect is called scuffing or galling.

The Archard wear law provides an expression for adhesive wear, According to Archard's law (1953) which describes the inverse relationship between the wear volume loss (*W*) and hardness (*H*) can be expressed as

$$W = k\frac{LS}{H} \tag{2.1}$$

Where $W$ is the wear volume loss, $k$ is a constant known as wear coefficient, $L$ is the normal load, $S$ is the sliding distance and $H$ is the hardness of softer materials (Archard 1953). **Abrasive wear** occurs when a harder material is rubbing against a softer material (Rabinowicz 1995). If there are only two rubbing parts involved in the friction process the wear is called two body wear. In this case the wear of the softer material is caused by the asperities on the harder surface. If the wear is caused by a hard particle (grit) trapped between the rubbing surfaces it is called three body wear. According to Stachowiak and Batchelor (2005) wear due to the mechanical interaction between a solid surface and a fluid, or impinging liquid or solid particles is called **erosive wear**. When particles with some velocity are impacted on the surface of metal, pits and large scale subsurface deformations occur on the metal surface. Wear caused by fracture arising from surface fatigue due to cyclic loading is called **fatigue wear.** It results in a series of pits or voids. It usually occurs in rolling or sliding contact bodies, such as bearings, etc. After repeated cyclic loading, a crack is observed on the subsurface or the surface. The subsurface cracks propagate, connect with other cracks, reach the surface and generate wear particles. **Corrosive wear** occurs when sliding takes place in a corrosive or oxidative environment as explained by Stachowiak and Batchelor (2005). During dry sliding also, the oxygen from the normal environment or other gases present in the environment can react with the solid surface. The excessive presence of anti-wear additives or other chemical agents can also cause corrosive wear. At elevated temperatures, oxygen can interact with a sliding surface and form oxides called oxidative wear.

## 2.7 Dry sliding wear of composite materials

When the wear of composites or metals is performed at room temperature in the absence of any lubricant, it is known as dry sliding wear. Exhaustive research has been carried out by many authors to explore the sliding wear behavior of copper composites under different conditions. Authors have mainly investigated the effect of sliding conditions like load, sliding velocity, initial surface roughness, mechanical properties, environmental etc., and the mechanism of wear operating under these conditions.

### 2.7.1 Factors affecting sliding wear composites

The wear properties of Cu-based sintered powder materials containing molybdenum disulfide and molybdenum diselenite using pin on disk apparatus at a sliding speed of 0.15 m/s and a contact pressure of 0.127–1 MPa was investigated by Kovalchenko et al. (2012). The unreinforced copper quickly began scuffing and eventually experienced a catastrophic failure in a short period of sliding time. Scuffing and catastrophic damage was prevented by incorporating $MoS_2$ and $MoSe_2$ into the copper using powder metallurgy technology. Material removal resulted from adhesion between the sliding composite materials and the transferred material on the copper counterface, which forms flaky debris. It was observed that the lubricating effect is more pronounced at concentrations greater than 5 wt.% of the solid lubricant.

Rajkumar et al. (2013) investigated the tribological behavior of copper–nano-graphite composites using pin-on-disk tribometer. The reinforced nano-graphite volume fraction is (5%, 10%, 15% and 20%). The normal loads were varied from 12 to 60 N and sliding speed were varied 0.77 to 2.77 m/s. In the experiment it was found that copper–nanographite composites showed higher wear resistance compared to copper–graphite composites. High surface area of nano-graphite particles embedded in copper matrix exhibited high adherent graphite tribo-layer at the contact surface. It was observed that operating wear mechanism for 5 vol.% nano graphite composite is oxidative with plastic deformation whereas 10–15 vol.% nano-graphite composite is oxidative with delamination.

The tribological characteristics of cast copper–$TiO_2$–boric acid hybrid composites were investigated by Ramesh et al. (2009). Loads were varied from 10 to 50 N and sliding velocities were varied from 0.3 to 1.2 m/s. They explored the effect of reinforcement, sliding speed and load on the copper and its hybrid composites. It was observed that wear rates of hybrid composites were lower when compared to copper. Increased content of hard reinforcement for a given volume fraction of soft reinforcement leads to lower wear rates of hybrid composites. It is observed that for all the materials studied, the wear rate increases drastically up to a sliding distance of 94 m. With further increase in sliding distance there is a steady increase in the wear rates. It is also observed that an increase in load results in increased wear rates for copper and its hybrid composites.

In another investigation by Ramesh et al. (2009) the tribological behavior of cast copper–SiC–Gr hybrid composites using pin on disk apparatus were studied. Wear studies were conducted at various loads ranging from 10 to 50 N. The sliding velocities were varied from 0.3 to 1.2 m/s. It is clearly observed that dispersion of silicon carbide a hard phase in copper matrix tends to reduce the wear rate of copper while use of graphite a soft phase as reinforcement in copper results in increased wear rate when compared with Cu–SiC composites. Increased content of hard reinforcement for a given volume fraction of soft reinforcement leads to lower wear rates of hybrid composites as compared to copper. It is pointed out that an increase in load results in increased wear rates for copper and hybrid composites.

Microstructural, mechanical and tribological behavior of aluminium nitride reinforced copper matrix composites were investigated by Thankachan et al. (2017). Sliding wear test were performed against a hardened chromium steel disc by using pin on disk machine at a load of 30 N and at a rotating velocity of 1 m/s for a distance of 1500 m. It was observed that wear resistance increased with the AlN reinforcement. Worn surface analysis showed that with AlN addition wear rate through adhesion has also reduced significantly.

Dhokey et al. (2008) explored the wear mechanisms in copper-based SiCp (20% by volume) reinforced composite using pin-on-disk machine at four loads (15 N, 25 N, 45 N, and 65 N) and four sliding speeds (0.6, 1.2, 1.8, 2.4 m/s). Using dimensional analysis approach, it is possible to indicate with clarity the mild regime and severe wear regime with a well defined transition point. Wear regime map provides basis for selecting optimum operating variables and also can be useful in locating working domain for practical application.

The wear and mechanical properties of sintered copper–tin composites containing graphite or molybdenum disulfide were studied by Kato et al. (2003). The wear properties of the materials were estimated by a cylinder-on-plate wear machine under dry conditions at room temperature in air. Graphite was very effective in reducing the wear of the composites. Furthermore, the wear rate of the Cu-coated graphite specimens was much lower than that of the uncoated graphite specimens. By contrast, the wear rates of the $MoS_2$ composites increased considerably with the amount of $MoS_2$ addition. This behavior is thought to be due to the absence of $MoS_2$ and the presence of brittle $CuMo_2S_3$ compounds in the sintered composites.

Tu et al. (2003) studied the dry sliding wear behavior of in situ Cu–$TiB_2$ nano composites against medium carbon steel using pin-on-disk wear tester under dry sliding conditions, rubbing against medium carbon steel disk at sliding speeds range from 0.089

to 0.445 $ms^{-1}$ and at loads between 20 and 140 N. Due to the good interfacial bonding between uniformly dispersed $TiB_2$ nano-particles and the copper matrix, there was no transition from mild wear to severe wear over the applied load range. The wear resistance made the material a potential candidate for sliding electrical contacts.

The wear behavior WC particle reinforced copper matrix composites using a pin-on-disk apparatus against a sintered SiC abrasive disk was investigated by Deshpande et al. (2006). It was observed that up to a normal load of around 9 N (or 0.55 MPa pressure), the wear rate of fully dense Cu/WC (53 vol.%) composites increases linearly with the applied pressure. Results also reveal that porosity in the Cu/WC composite increases wear.

Xiao et al. (2017) investigated the dry sliding wear behavior of Cu-$MoS_2$ composite pins against bearing steel (AISI 52100) discs. The $MoS_2$ content ranged from 0–40 vol.%. The tests were conducted at a constant normal load of 5 N, a rotational speed of 200 rpm (0.42 m/s) and a fixed sliding distance of 15 km. The wear rates of the composites first increases and then decrease as the $MoS_2$ content increases. The high wear rates of Cu-5 vol% $MoS_2$ and Cu-10 vol.% $MoS_2$ composites are mainly attributed to the cracks associated with the $MoS_2$ particles, and the decrease of wear rate for composites with $MoS_2$ above 20 vol.% is derived from the formation of a nearly continuous lubricating film on the worn surface.

The friction and wear of copper–graphite composites with graphite contents of 8, 15, and 20 wt. % made by powder metallurgy route using either Cu-coated graphite powders or mixture of copper and graphite powders were explored by Moustafa et al. (2002). The wear testing was carried out using a pin-on-ring tribometer at a speed of 0.2 $ms^{-1}$ and the applied normal load varied from 50 to 500 N. It was found that composites made by Cu-coated and uncoated graphite have lower wear rates than those made from pure copper. The wear mechanisms of pure copper compacts at each wear rate regime were believed to be oxidation–delamination, delamination, and seizure wear mechanisms, whereas the involved wear mechanisms of either of composites were the same, and they were oxidative-dominant, strain-induced delamination, and sub-surface delamination.

Mirazimi et al. (2016) investigated the dry sliding wear behavior of yttria stabilized zirconia (YSZ) reinforced Cu matrix composite specimens using pin on disk. The volume loss and wear rate of pure Cu specimen were 1.48 $mm^3$ and $1.5\times10^{-3}$ $mm^3/m$ under 50 N applied load and 1000 m sliding distance. However, for composite containing 5% YSZ particles these values dropped to 0.97 $mm^3$ and $0.9\times10^{-3}$ $mm^3/m$, respectively. The worn surface and debris analysis indicates that local plastic deformation and delamination as dominant wear mechanisms for pure copper, while oxidation and ploughing for composite specimen.

The sliding wear behavior of SiC-particle reinforced copper matrix composites fabricated by sintering and sinter-forging processes was studied by Shabani et al. (2016). The disk was rotated at 18 mm/s, and the normal loads were 15, 35 and 55 N. The duration and sliding distance of wear test was 2 h and 132 m; respectively. The dry sliding wear tests represented that the sinter-forged Cu composite compacts with 60 vol.% SiC exhibit the lowest wear loss compared to other compacts due to its better hardness properties.

Fathy et al. (2012) investigated the abrasive wear properties of Cu–$Al_2O_3$ nano-composite using a pin-on-disk technique under normal loads of 2, 4, 6 and 8 N, at four different sliding speeds; 0.91, 1.07, 1.21 and 1.62 m/s, and four different alumina weight fractions (0%, 2.5%, 7.5%, and 12.5%). It was observed that the wear rates of the nanocomposites increased with increasing applied loads or sliding speed. The wear rate of the monolithic copper is more than that of the nanocomposites.

Alaneme et al. (2017) investigated the mechanical and wear behavior of copper matrix composites reinforced with steel chips by using Taber abrasion machine. The mechanical properties (hardness and tensile properties) and wear resistance were observed to improve with the use of the steel machining chips as reinforcement.

The wear mechanism of copper matrix composites reinforced with SiC and graphite particles were explored by Zhan et al. (2004). Dry sliding wear tests were conducted using a block-on-ring type wear machine at a constant sliding velocity of 0.42 m/s. The normal loads were 20, 50, and 110 N. The results indicate that a graphite-rich mechanically mixed layer (MML) formed on the tribo-surface was responsible for the good tribological properties of the hybrid composites at low normal loads. When graphite content was high enough for delamination wear to take place at high load, wear resistance deteriorated.

The wear behavior of new lead free metal matrix composite, centrifugally cast copper alloy graphite (C90300-10%graphite) composite (CG) in comparison to a commonly used leaded copper (LC) alloy (18-22% Pb) were studied by Kestursatya et al. (2003). Tribological tests were conducted with pins made from these materials and tested against a SAE 1045 steel counter face in the load range of 27-118 N. It was observed that wear loss of the centrifugally cast C90300-10% graphite pins were considerably lower than the normalized wear loss of the leaded copper alloy. Mutual material transfer between the pin and the disk was observed in both CG-steel and LC-steel. With increase in the applied load the amount of material transfer from the pin to the surface of the disk increased for both LC and CG materials.

The wear behaviors of $(Ni_3Al)p$ reinforced Cu matrix composites were studied by Celikyurek et al. (2011). The dry sliding wear tests were performed with pin-on-disk geometry (CSM Tribometer) at 0.5 and 1 $ms^{-1}$ sliding speed under 10 N normal load and ambient atmosphere in humidity of 40%. The wear resistance of the composites was considerably improved with an addition of $Ni_3Al$. With the addition of $Ni_3Al$ to copper, the direct copper- counterface contact was reduced that resulted in the increase of wear resistance. The EDS analyses of worn surface show that there is material transfer from counter disk to sample pin for composites and the existence of oxygen confirms that oxidation occurred on the interface during sliding.

The tribological behavior of SiC particle-reinforced copper matrix composites by using pin-on-disk tester were analyzed by Tjong et al. (2000). The abrasive wear measurements showed that soft copper exhibits an extremely high wear loss. However, additions of SiC particles up to 20 vol. % appeared to improve the abrasive wear resistance of copper significantly under the applied loads of 15–55 N. Dry sliding wear tests also indicated that the composite with 20 vol. % SiC exhibits a lower wear loss compared to pure copper. This was due to the reinforcing SiC particles being effective to reduce the extent of wear deformation in the subsurface region during sliding.

Gautam et al. (2008) explored the tribological behavior of Cu–Cr–SiCp in situ composite by using pin on disk apparatus under a normal load range between 10 and 40 N and at sliding a fixed speed of 0.786 $ms^{-1}$. It was observed that the cumulative volume loss of the cast composite decrease to about 65% and 72%, respectively, as compared to those observed in as-received copper and cast copper at 40 N loads.

In an another study by Gautam et al. (2011) the dry sliding wear behavior of hot forged and annealed Cu–Cr–graphite in-situ composites were investigated. In this investigation Cu based composites were developed by stir casting method by adding fixed amount of Cr (4 wt.%) and different amounts of graphite viz. 2, 3 and 4 wt.%. Dry sliding friction and wear behavior of all the composites in as cast, hot forged and annealed conditions has been performed by sliding against a counter-face of SAE 4615 steel disc under ambient conditions using a pin-on-disk machine at a normal loads 10, 20, 30, and 40 N and a constant sliding speed of 0.786 m/s. It was observed that volume loss increases linearly with increasing sliding distance for all materials. The wear rate increases linearly with increasing normal load. Wear rate of Cu–4Cr–4G composite is significantly lower than that of all other materials either hot forged or annealed. From the worn surface analysis of the pin specimen it was revealed that significant formation of transfer layer occurs on hot forged and annealed Cu–4Cr–4G composite.

### 2.7.2 Sliding wear of Cu-TiC composites

The dry sliding wear properties of Cu-TiC composites under different operating conditions were reported by authors.

The mechanical properties and tribological characteristics of Cu-TiC composites prepared by powder metallurgy route were studied by Akhtar et al. (2009). It was observed that sintered density and other mechanical properties increases considerably by the addition of titanium carbide content and alloying elements in the copper matrix phase. In this study, the wear resistance of the composites was done against high speed steel at an applied load of 150 N and 300 N. Less microploughing and wear loss was observed at lower loads and high vol.% of TiC particles whereas intense micro-ploughing was observed under 300 N load.

The microstructure and wear properties of Cu–TiC composite developed by friction stir processing were studied by Sabbaghian et al. (2014). A pin-on-disk apparatus (WC counterpart) was employed for the wear test under the load of 50 N, rotational pin speed of 2430 mm/min, traversal radius of 10.18 mm, and the total distance of 250 m. It was observed that increasing TiC reinforcement resulted in a higher hardness and reduced wear rate because of the good bonding between the reinforcing particles with base metal. Wear resistance of composites was done against the WC counterpart at 50 N load and it was found that the weight loss and wear rate of the composite specimen are less than those of pure copper. This is due to the high hardness of the composite layer and decrease in contact between the specimen surface and pin due to the presence of TiC particles.

The tribological behavior of copper–TiC–graphite hybrid composites under testing parameters of normal loads 12–48 N and sliding speed of 1.25–2.51 m/s was explored by Rajkumar et al. (2011). It was observed that wear rate of hybrid composites reduced with increasing TiC percentage and graphite percentage, due to the mutual effect offered by both the reinforcements. The formation of mixed smooth layer with higher graphite hybrid composites enhances the wear resistance. Increasing sliding velocity from 1.25 to 2.51 m/s were marginally increasing wear rate of hybrid composites. Oxidative wear is dominant wear mechanism for hybrid composites.

The tribological performance of Cu hybrid composites reinforced with graphite and TiC were analyzed by Nayak et al. (2014). The wear resistance of the Cu hybrid composites increased with graphite content. An increase in graphite content resulted in delamination wear and a decrease in abrasive wear. The wear loss of hybrid composites was reduced with increasing TiC and graphite content due to the combined effect offered by both the reinforcements. FESEM studies of the worn surfaces and wear debris revealed that the wear mechanism for the Cu-10TiC-5Gr hybrid composite was oxidative wear with plastic deformation. The wear mechanism operating in Cu-10TiC-15Gr hybrid composites was oxidative wear along with delamination.

Zhuang et al. (2010) investigated the influence of technological process on dry sliding wear behavior of titanium carbide reinforced copper matrix composites. Two types of milled process are used in SPS to prepare TiC reinforced Cu matrix composites: (a) Ti and C powders are milled together, and then mixed with Cu powders; (b) All the three kinds of powders are milled together. The dry sliding wear tests were conducted in air at room temperature with a pin-on disk test rig and GCr15 steel disc with a hardness of about 55 to 58 HRC was employed as counterpart. The applied loads were 20, 60, 100, 140 and 200 N, and the sliding speed was 0.63 m/s. It was observed that as the load increases the wear rate decreases sharply up to 60 N and then decreases linearly. All the composites exhibit good wear resistance at 200 N normal load with lowest wear loss $1.4\times10^{-5}$ $mm^3$/Nm (method (a)) and $1.12\times10^{-5}$ $mm^3$/Nm (method (b)) respectively. The composites made by method (a) show third-body abrasion with mechanical mixed layer, but the composites made by method (b) exhibits plastic deformation on worn surface.

In another investigation Zhuang et al. (2011) developed Cu-TiC composites by mechanical alloying and spark plasma sintering. The dry sliding wear tests were conducted with a pin-on-disk wear testing machine, and GCr15 steel disc was employed as counterpart. The applied loads were 20, 60, 100, and 200N with 0.63 m/s speed. From the investigation it was observed that specific wear loss decrease sharply as increase of normal load from 20 N to 60 N, specific wear loss from $18.75\times10^{-5}$ $mm^3$/Nm to $2.27\times10^{-5}$ $mm^3$/Nm, and then decrease linearly following the enhancement of normal load. It was pointed out that third body abrasion is primary wearing mechanism in wear test. From the SEM analysis of worn surfaces the formation of mechanical mixed layer can be observed which reduces the specific wear loss of the composites.

Dry sliding wear properties of Cu-TiC composite developed by reduction sintering and cold extrusion process were explored by Vu et al. (2012). TiC content was varied from 1 to 5 wt.% in the copper matrix. The wear test was conducted at room temperature using a Tribotester (France) at 18 N load. It was observed that the wear rate reduces with TiC content up to 5 wt.%. The results also show that the wear resistance of sample subjected to cold extrusion has lower than that of reduction sintering at the same

TiC content. From SEM analysis it was revealed that the formation of oxide layer appeared on the wear surface of the sample and it results in the reduced wear resistance.

## 2.8 Predictions of wear properties using response surface methodology

Response surface methodology is a compilation of mathematical and statistical techniques that are used for modeling and establishing the relationships between the process parameters and responses with a minimum number of experiments (Montgomery 1997). RSM is useful because of the following salient features as suggested by Ross (1996) and Ezilarasan (2011):

a) Visualization of the relationship between one or more responses and a number of independent variables that influence the responses.
b) Finding and exploring the optimum operating conditions for the system, or determining a region of the factor space in which operating specifications are satisfied.
c) Finding appropriate robust designs that can be effectively used for the purposes of objectives and finding robust conditions which produce the product with robust quality characteristics.

The extensive applications of RSM are in the particular situations where several input variables significantly influence the performance measure or quality characteristics of the process. In order to find out the relationship between the process parameters and the responses, second order polynomial response surface mathematical models can be considered as

$$Y_u = b + \sum b_i x_{iu} + \sum b_{ii} x^2_{iu} + \sum b_{ij} x_{iu} x_{ju} \qquad (2.2)$$

where $Y_u$ is the response variable whereas b, $b_i$, $b_{ii}$ and $b_{ij}$ are the coefficients. In the above polynomial equation the second term under summation sign denotes the linear effect, the third term corresponds to the higher order effect and the fourth term is attributed to the interaction effect. It was found that the face centered central composite design (CCD) is very well fitted to the second order response surface. Face centered central composite design finds importance over the entire design space because it provides comparatively high quality prediction. The design was developed and analyzed using MINITAB 16 statistical package.

Grumet al. (2004) explained that the RSM is quite helpful in developing a suitable estimate for the true functional relationship between the independent variables and the response variable that may characterize the nature of the machining. It has been proved that efficient use of statistical design of experimental techniques, allows the development of an empirical methodology to incorporate a scientific approach.

RSM provides quantitative measurements of possible interactions between factors to obtain difficult information using other optimization techniques. Detection and quantification of the interactions between various factors are of critical importance especially for multivariate optimization in engineering problems and application of RSM in the prediction of the process characteristics as discussed by Donglai et al. (2008).

Various authors have used RSM to optimize their process parameters and to know the effect of process parameters on the responses. In an investigation by Yigezu et al. (2013) statistical model were used to investigate the effect of applied load, sliding distance and weight percentage of reinforcement on the wear behavior of TiC reinforced Al matrix composites produced via stir casting route. The experimental results showed that the sliding distance and weight percentage of TiC had relatively higher effect on coefficient of friction whereas the applied load had relatively higher influence on the weight loss. The developed regression equations for predicting the weight loss and coefficient of friction were validated with a number of test cases and it has been observed that the percentage error for both responses is less than ± 10%.

In another work by Nayak et al. (2104) the graphite (5, 10, and 15 vol.%) and TiC (5, 10, and 15 vol.%) reinforced copper hybrid metal matrix composite were prepared by using powder metallurgy. They explored the effect of process parameters such as graphite percentages, load, sliding speed, and sliding distance on the sliding wear behavior of the hybrid composites based on the design of experiments. Analysis of variance (ANOVA) was used to investigate the effect of the process parameters on the wear weight loss. It was observed that normal load has greater influence on the weight loss.

The dry sliding wear properties of Al–Si12Cu/$TiB_2$ metal matrix composite using response surface methodology were investigated by Radhika et al. (2015). In this study a plan of experiment based on five-level central composite design (CCD) using response surface methodology was developed. The process parameters considered for the experiments are load, velocity and sliding distance and the response variable is wear rate. The obtained mathematical model showed the relation between the process parameters with the response and predicts the wear behavior of the composites.

The wear behavior of particulate and fiber-reinforced nano-ZnO/ultra-high molecular weight polyethylene hybrid composites by response surface methodology was studied by Chang et al. (2014). Pin-on-disk tester was used to analyze its wear properties under diverse operating conditions of applied loads, sliding speeds and sliding distances. Analysis of variance (ANOVA) was used to obtain the mathematical regression models of the wear volume and average coefficient of friction. The mathematical models revealed that applied load, sliding speed and distance have major influence on the wear and friction properties of both ultra high molecular weight polyethylene composites.

Study of the sliding wear behaviors of Al-7075 alloy and Al-7075 hybrid composite using the response surface methodology were reported by Kumar et al. (2015). They observed that load is major factor which influence the specific wear rate while sliding speed and sliding distance has minor effect on the wear rate.

Vettivel et al. (2013) worked on the wear map and modeling of extruded tungsten reinforced copper composite by using design expert software. It was found that hardness of the composite increases with increment in tungsten content. The specific wear rate is deteriorated with increasing sliding distance. The wear rate map is established to illustrate the wear state with respect to the load, sliding distance and percentage of tungsten.

The use of full factorial design to optimize the wear test conditions of the copper-multi-walled carbon nano-tubes and nano boron carbide reinforced composites developed via powder metallurgy were reported by Gangatharan et al. (2016). Boron carbide particle, applied load and sliding distance were taken as process variables. The ANOVA results shows that the applied load and nano boron carbide addition to the matrix material especially plays a vital role in the wear resistance and coefficient of friction of the hybrid composites.

Kumar et al. (2013) used the full factorial design of experiment based abrasive wear modeling of in- situ Al–4.5% Cu/x TiC (where x=5%, 7% and 10% wt.%) metal matrix composites. Wear test of the composites were done by using a pin-on-disk apparatus. The control factors were the applied load, sliding distance and weight% of TiC reinforcement in the metal matrix. It has been observed from the main effect plots that the significance of sliding distance on weight loss is relatively higher than the applied load and weight% of TiC. The interaction of load and sliding distance indicated significant effect on weight loss. It has also been observed that with a rise in the sliding distance coefficient of friction increased.

Suresh et al. (2014) studied the mechanical behavior and predicted the wear properties by using RSM. Mathematical models were developed between the key process parameters namely weight percentage of $TiB_2$, load and sliding distance and total experimental time were reduced. Analysis of Variance technique was applied to check the validity of the developed model. The mathematical model developed for the specific wear rate was predicted at 99.5% confidence level and some useful conclusions were made.

Sharma et al. (2016) optimized the wear properties of Al6082/Gr metal matrix composites by using response surface methodology. Percentage reinforcement, load, sliding speed and sliding distance were taken as the process variable. Analysis of Variance technique was applied to check the validity of the developed model. Results showed that sliding distance is the most influential factor and load is the factor which affects the wear least.

Mandal et al. (2012) investigated the wear behavior of 6061 Al-alloy/SiC with 10 vol.%SiCp . $2^3$ factorial designs of experiments were carried out to see the effect of few parameters, i.e., contact stress, speed and duration with respect to wear. A mathematical model were developed using regression analysis technique for prediction of wear behavior of the MMC and adequacy of the model were validated using analysis of variance (ANOVA) techniques. The results revealed that response surface methodology (RSM) is an effective tool for prediction of wear behavior under combined sliding and rolling action.

### 2.9 Formulation of the problem

From the above literature review it is observed that very limited work has been done on the synthesis of TiC-reinforced copper-based composites and their tribological behavior and still there is ample scope toward development of Cu-TiC composites by using powder metallurgy route. Therefore, the main objective of the present investigation is to synthesize the Cu-based composites containing different amounts of TiC by using Ni as the binding agent. It is clearly observed that Ni helps to increase bonding strength between copper and TiC particles because it is known that copper behaves predominantly as a donor rather than as an acceptor of electrons. TiC also behaves as a donor of electrons, so a high wetting angle can be expected for the Cu-TiC system. On the other hand, nickel with its incomplete 3d orbital acts as an acceptor of electrons (Chrysanthou 1996). Thus, the present investigation has been carried out to develop TiC reinforced Cu-4wt.% Ni matrix composites and to study its physical, mechanical and tribological properties with following objectives:

- To synthesize Cu-4wt. % Ni matrix composites reinforced with different percentages of TiC (0, 2, 4, 6, and 8 wt. %) through high energy ball milling followed by compaction and sintering.
- To analyze the compressibility behavior of the milled powders by using Panelli and AmbrosioFilho, Heckel and Ge compaction equations.
- To evaluate the friction and wear performance by conducting sliding wear tests under different loads using a pin-on-disk machine. The study also aims to correlate the observed wear behavior with the mechanical properties and to explore the operative mechanism of wear during sliding of these composites.
- Optimization of wear properties of the composites will be performed by using response surface methodology (RSM).